Pergamon

Int. J. Solids Structures Vol. 35, No. 16, pp. 1981–1999, 1998

0020–7683/98 $19.00 + .00

PII: S0020–7683(97)00165–0

A BOUNDARY CONTOUR FORMULATION FOR DESIGN SENSITIVITY ANALYSIS IN TWO-DIMENSIONAL LINEAR ELASTICITY

ANH-VŨ PHAN
Department of Mechanical Engineering, Ecole Polytechnique, Montréal, Québec, Canada H3C 3A7

SUBRATA MUKHERJEE
Department of Theoretical and Applied Mechanics, 212 Kimball Hall, Cornell University, Ithaca, NY 14853, U.S.A.
E-mail: sm85@cornell.edu

J. R. RENÉ MAYER
Department of Mechanical Engineering, Ecole Polytechnique, Montréal, Québec, Canada H3C 3A7

(*Received* 29 *January* 1997; *in revised form* 25 *May* 1997)

Abstract—A formulation for computing first-order shape design sensitivities in two-dimensional (2-D) linear elastostatics by the boundary contour method (BCM), along with a numerical implementation using quadratic boundary elements, is presented in this paper. Here, the direct differentiation approach is analytically applied to the appropriate boundary contour equations in order to derive the sensitivities of all the physical quantities (displacements, tractions and stresses) on the boundary as well as those for displacements and stresses inside the body under consideration. The nonsingular formulation of the BCM is used for computing the boundary displacements, and boundary stresses at "off contour" regular points. A regular boundary point is a point on the boundary where it is locally smooth; an off contour point lies inside a boundary element. Their corresponding sensitivities are obtained in a straightforward manner from the resulting regular sensitivity formulation. Also, the stress sensitivities at the boundary nodes can be recovered easily from the global displacement shape functions described in a Cartesian coordinate system. Finally, through three numerical examples for which analytical solutions exist, it is shown that the BCM can provide remarkably accurate numerical results for shape sensitivities. © 1998 Elsevier Science Ltd.

1. INTRODUCTION

The conventional boundary element method (BEM) for linear elasticity requires the numerical evaluation of line integrals for two-dimensional (2-D) problems and surface integrals for three-dimensional (3-D) ones [see, for example, Mukherjee (1982); Banerjee (1994)]. By observing that the integrand vector of this boundary integral equation (BIE) without body forces is divergence free, Nagarajan *et al.* (1994, 1996) have proposed a novel approach, called the BCM, that achieves a further reduction in dimension. The divergence free property allows, for 3-D problems, the use of Stokes' theorem to transform surface integrals on the usual boundary elements into line integrals on the bounding contours of these elements. For 2-D problems, a similar transformation eliminates numerical integration altogether. The above transformations are quite general and apply to boundary elements of arbitrary shape. Thus, the BCM requires only numerical evaluation of line integrals for 3-D problems and simply the evaluation of functions (called potential functions) at points on the boundary of a body for 2-D cases.

The BCM is a young method and further developments of this approach are under way. A hypersingular BCM (HBCM) formulation for linear elasticity has been proposed recently (Mukherjee and Mukherjee, 1997; Phan *et al.*, 1997b). This formulation can possibly be extended to solve fracture mechanics problems. It is pointed out in Nagarajan *et al.* (1994) that the divergence free property of the BEM integrand holds true for other linear problems besides potential theory and linear elasticity. Thus, in principle, it is possible

to derive BCM formulations for other linear problems such as plate bending, transient heat conduction with uniform initial temperature, and thermoelasticity; although such formulations have not been derived yet. Finally, body forces that can be modeled as particular integrals in the usual BEM [see, for example, Banerjee (1994)] can also be modeled in the same way by the BCM. Thus, at least in principle, the BCM is a fairly general approach for linear problems. The method, however, is not recommended for nonlinear problems, since the primary advantage of a further reduction in dimension, compared to the usual BEM, would, in general, be lost in these cases.

Most shape optimization problems employ mathematical programming methods where design sensitivity coefficients (DSCs), which are defined as the rates of change of physical response quantities with respect to changes in the design variables, are required for determination of the optimum shape of a body.

Unlike the well-known finite element method (FEM), the boundary element method (BEM) requires only discretization on the boundary of a body. This characteristic provides significant advantages in its use in shape optimal design where mesh generation needs to be redone after each iterative step of the optimization process. Therefore, several researchers have used the BEM to develop efficient approaches for computing design sensitivities. The reader is referred to a special issue of *Engineering Analysis with Boundary Elements* (Bui and Bonnet, 1995) for a recent discussion of sensitivity analysis with the BEM. As in the context of the FEM, there are three methods [e.g. Haug *et al.* (1986); Sokolowski and Zolesio (1992)], namely, the finite difference approach (FDA), the adjoint structure approach (ASA) and the direct differentiation approach (DDA).

Besides having the same advantage in mesh generation as for the conventional BEM, the BCM offers a further reduction in dimension, and especially, a nonsingular formulation for computing boundary displacements and boundary stresses at regular points inside a boundary element [see Phan *et al.* (1997a)]. Moreover, the stresses at boundary nodes can be recovered easily and exactly from the global displacement shape functions expressed in Cartesian coordinates. These advantages of the BCM are expected to make it very competitive in optimal shape design.

To that purpose, this paper presents a formulation for computing first-order design sensitivities based on a full development of the BCM for 2-D linear elasticity with quadratic boundary elements which has been introduced by Phan *et al.* (1997a). In this paper, we develop a formulation for design sensitivities by direct differentiation of the BCM equations, i.e. by using the DDA. In the context of the BEM for elastostatics, the DDA has been used by Barone and Yang (1988), Kane and Saigal (1988), Zhang and Mukherjee (1991), and Mellings and Aliabadi (1995) for 2-D problems, by Saigal *et al.* (1989), and Rice and Mukherjee (1990) for axisymmetric problems, by Aithal *et al.* (1991), Kane *et al.* (1992) and Bonnet (1995) for 3-D bodies, and by Mukherjee and Chandra (1991), and Chandra and Mukherjee (1997) for 2-D nonlinear problems.

The DDA may be applied either before or after discretization of the initial BIE. The two processes are expected to lead to the same equations. Kane and Saigal (1988) generated the desired DSCs by differentiating the resulting BEM system matrix analytically. In these formulations, the authors have placed the source points outside the region to avoid singular integrations. Barone and Yang (1988) carried out the opposite process by differentiating the BIE to obtain the DSCs analytically before numerical integration. Here, the rigid body motion technique has been employed to treat singular integral terms in the calculation of displacement sensitivities, but the integration of strongly singular kernels is required in a direct formula used in computing stress sensitivities. Zhang and Mukherjee (1991) overcame this difficulty related to the singular feature of the governing BIE by using a 2-D elastic BIE formulated in terms of tangential gradient of displacements where the sensitivity of boundary stresses is recovered from the corresponding tractions and tangential gradients of displacements and their sensitivities. In order to avoid strongly singular integrals involved in design sensitivity analysis, Bonnet (1995) applied the material derivative concept to the regularized displacement boundary integral equation.

It can be seen from the above papers that most authors limit their calculations to design sensitivities on the boundary of a body. The formulation described in this work

includes the DSCs of all displacements and stresses throughout the domain of interest, i.e. on the boundary as well as inside the body. DSCs are obtained from completely regularized equations. There is no need to evaluate any singular integrals as in the BEM work of Barone and Yang (1988). In fact, for 2-D linear elasticity, the BCM does not require the numerical evaluation of any integral at all!

Three examples, including Lamé, Kirsch and a plate with an elliptical cutout, are solved and compared against analytical solutions. The numerical results are very accurate for these illustrative examples.

2. 2-D BCM FORMULATIONS

The information presented in this section is summarized from Phan *et al.* (1997a) where more details can be found.

2.1. *Basic formulation*

The idea of dimensional reduction starts from the standard boundary integral equation (BIE) without body forces [see Rizzo (1967)]

$$c_{ik}(P)u_i(P) = \int_{\partial B} [U_{ik}(P, Q)\sigma_{ij}(Q) - \Sigma_{ijk}(P, Q)u_i(Q)]\mathbf{e}_j \cdot \mathrm{d}\mathbf{S} \tag{1}$$

where c_{ik} is the corner tensor, P, Q, u_i and σ_{ij} are the source point, field point, displacement vector and stress tensor respectively, U_{ik} and Σ_{ijk} are the Kelvin kernel tensors (Rizzo, 1967), and $\mathbf{e}_j$ are global Cartesian unit vectors. In 2-D problems, ∂B is the boundary of a body B, and $\mathrm{d}\mathbf{S}$ is an infinitesimal boundary length vector.

Let $\mathbf{F}_k = [U_{ik}(P, Q)\sigma_{ij}(Q) - \Sigma_{ijk}(P, Q)u_i(Q)]\mathbf{e}_j$. Since the divergence of $\mathbf{F}_k$ at a field point Q is zero [see Nagarajan *et al.* (1994)], i.e.

$$\nabla_Q \cdot \mathbf{F}_k = 0 \tag{2}$$

everywhere except at the source point P, so after discretizing the boundary ∂B into n elements, the BIE (1) can be converted to the following BCM version

$$c_{ik}(P)u_i(P) = \sum_{\ell=1}^{n} [\Phi_k^{(\ell)}(E_{\ell 2}) - \Phi_k^{(\ell)}(E_{\ell 1})]. \tag{3}$$

Here, $E_{\ell 1}$ and $E_{\ell 2}$ are the endpoint nodes of element (ℓ), and Φ_k are called the main potential functions that are determined by solving the following identity that satisfies eqn (2)

$$\mathbf{F}_k = \frac{\partial \Phi_k}{\partial y}\mathbf{e}_1 - \frac{\partial \Phi_k}{\partial x}\mathbf{e}_2. \tag{4}$$

A numerical implementation of eqn (3) does not require any numerical integration.

2.2. *Formulation using the rigid body motion technique*

In order to regularize Cauchy singular integrals in eqn (1), a rigid body motion solution is applied to this equation to produce a new equation

$$\int_{\partial B} \{U_{ik}(P, Q)\sigma_{ij}(Q) - \Sigma_{ijk}(P, Q)[u_i(Q) - u_i(P)]\}\mathbf{e}_j \cdot \mathrm{d}\mathbf{S} = 0. \tag{5}$$

Since the new integrand vector $\mathbf{G}_k = \{U_{ik}(P, Q)\sigma_{ij}(Q) - \Sigma_{ijk}(P, Q)[u_i(Q) - u_i(P)]\}\mathbf{e}_j$ is

still divergence free (everywhere except at P), eqn (5) can be converted to the following corresponding BCM version

$$\sum_{\ell=1}^{n} [\Psi_k^{(\ell)}(E_{\ell 2}) - \Psi_k^{(\ell)}(E_{\ell 1})] = 0 \tag{6}$$

where Ψ_k is determined by solving the following identity

$$\mathbf{G}_k = \frac{\partial \Psi_k}{\partial y}\mathbf{e}_1 - \frac{\partial \Psi_k}{\partial x}\mathbf{e}_2. \tag{7}$$

2.3. *Implementation with quadratic boundary elements*

Quadratic shape functions that ensure the divergence free property of $\mathbf{F}_k$ and $\mathbf{G}_k$ are given by

$$\begin{Bmatrix} u_1 \\ u_2 \end{Bmatrix} = \beta_1 \begin{Bmatrix} 1 \\ 0 \end{Bmatrix} + \beta_2 \begin{Bmatrix} x \\ 0 \end{Bmatrix} + \beta_3 \begin{Bmatrix} y \\ 0 \end{Bmatrix} + \beta_4 \begin{Bmatrix} 0 \\ 1 \end{Bmatrix} + \beta_5 \begin{Bmatrix} 0 \\ x \end{Bmatrix} + \beta_6 \begin{Bmatrix} 0 \\ y \end{Bmatrix} + \beta_7 \begin{Bmatrix} x^2 \\ k_2 xy \end{Bmatrix} + \beta_8 \begin{Bmatrix} y^2 \\ k_1 xy \end{Bmatrix} + \beta_9 \begin{Bmatrix} k_1 xy \\ x^2 \end{Bmatrix} + \beta_{10} \begin{Bmatrix} k_2 xy \\ y^2 \end{Bmatrix} \tag{8}$$

where $k_1 = -2(1-2\nu)$, $k_2 = -4(1-\nu)$ and ν is the Poisson's ratio.

In matrix form, for element (ℓ)

$$\{u^{(\ell)}\} = [T_u^{(\ell)}(x, y)]\{\beta^{(\ell)}\} \tag{9}$$

where $\{\beta^{(\ell)}\} = \langle \beta_1^{(\ell)} \beta_2^{(\ell)}, \ldots, \beta_{10}^{(\ell)} \rangle^{\mathrm{T}}$.

The configuration of a chosen quadratic boundary element is shown in Fig. 1. The relationship between the physical variable vector $\{p^{(\ell)}(x, y)\}$ and the artificial variable vector $\{\beta^{(\ell)}\}$ of boundary element (ℓ) are

$$\begin{aligned} \{p^{(\ell)}\} &= \langle u_1^{(2\ell-1)} u_2^{(2\ell-1)} \tau_1^{(2\ell-1)} \tau_2^{(2\ell-1)} u_1^{(2\ell)} u_2^{(2\ell)} \tau_1^{(2\ell)} \tau_2^{(2\ell)} u_1^{(2\ell+1)} u_2^{(2\ell+1)} \rangle^{\mathrm{T}} \\ &= [T^{(\ell)}(x, y)]\{\beta^{(\ell)}\}. \end{aligned} \tag{10}$$

A new coordinate system (ξ, η) centered at each source point is introduced. Equation (9) becomes

$$\{u^{(\ell)}\} = [T_u^{(\ell)}(\xi, \eta)]\{\hat{\beta}^{(\ell)}\}. \tag{11}$$

In eqn (11)

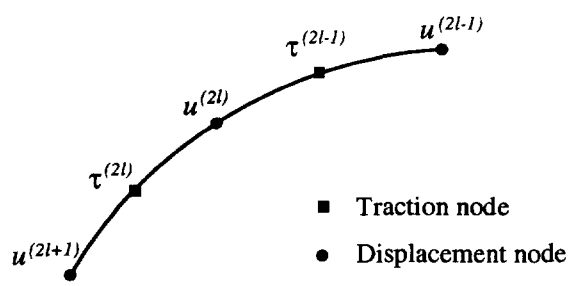

Fig. 1. Quadratic boundary element.

$$\{\hat{\beta}^{(\ell)}\} = [B_j]\{\beta^{(\ell)}\} \tag{12}$$

where $[B_j]$ is a matrix depending only on the coordinates of the source point j (since it arises from a coordinate transformation from the global system (x, y) to a system (ξ, η) centered at j).

3. DESIGN SENSITIVITY ANALYSIS

3.1. *Notation*

If the boundary ∂B of a 2-D body B is discretized into n boundary elements, then there are n endpoint nodes. Corners are always endpoint nodes. For convenience, let us define

- The boundary ∂B^* as the set of points belonging to the boundary ∂B except the n endpoint nodes. In other words

$$\{\text{The whole boundary } \partial B\} \equiv \{\text{The boundary } \partial B^*\} \cup \{n \text{ endpoint nodes}\}.$$

- The domain B^* as the set of points belonging to the body B except these n endpoint nodes, i.e.

$$\{\text{The whole domain } B\} \equiv \{\text{The domain } B^*\} \cup \{n \text{ endpoint nodes}\}.$$

3.2. *Boundary displacement sensitivities at displacement nodes and traction sensitivities at traction nodes*

As seen in the earlier work by Phan *et al.* (1997a) the numerical implementation of eqn (6) leads to

$$\left\{\sum_{\ell=1}^{n} [\Psi_k^{(\ell)}(E_{\ell 2}) - \Psi_k^{(\ell)}(E_{\ell 1})]\right\} = \sum_{\ell=1}^{n} [M^{(j\ell)}]\{p^{(\ell)}\} = \{0\} \tag{13}$$

where

$$[M^{(j\ell)}] = [\Psi^{(j\ell)}][B_j][T^{(\ell)}]^{-1} \tag{14}$$

in which $[\Psi^{(j\ell)}]$ is the matrix associated with the main potential functions Ψ_k and is evaluated at a source point j in the coordinate system (ξ, η).

The DSCs under consideration can be found by differentiating eqn (13) with respect to a design variable b, which is a typical component of a shape design vector $\mathbf{b}$. We have

$$\sum_{\ell=1}^{n} ([\overset{*}{M}{}^{(j\ell)}]\{p^{(\ell)}\} + [M^{(j\ell)}]\{\overset{*}{p}{}^{(\ell)}\}) = \{0\} \tag{15}$$

where $(^*)$ denotes the total derivative with respect to b, i.e. $(^*) = \mathrm{d}(\ )/\mathrm{d}b$ and generally,

$$(^*) = (\ )_{,b} + v_i(\ )_{,i}. \tag{16}$$

It is noted here that in order to avoid any ambiguities that might result from the use of the above notation for the total derivative of a long expression, the alternative notation $(\ )^*$ is used in such cases.

In eqn (16), the quantities $v_i = \mathrm{d}x_i/\mathrm{d}b$ are the components of the design velocity field. For 2-D cases, $x_1 \equiv x$ and $x_2 \equiv y$, thus eqn (16) can be expanded to

$$(\overset{*}{}) = (\ )_{,b} + (\ )_{,x}\overset{*}{x} + (\ )_{,y}\overset{*}{y}. \tag{17}$$

This total derivative is totally analogous to the concept of the material derivative (often taken with respect to time) in continuum mechanics.

It can be proved that $[\overset{*}{\Psi}^{(j\ell)}] = [\overset{*}{\Phi}^{(j\ell)}]$ ($[\Phi^{(j\ell)}]$ is the matrix associated with the main potential functions Φ_k), therefore, eqn (14) leads to

$$[\overset{*}{M}^{(j\ell)}] = [\overset{*}{\Phi}^{(j\ell)}][B_j][T^{(\ell)}]^{-1} + [\Psi^{(j\ell)}][\overset{*}{B}_j][T^{(\ell)}]^{-1} + [\Psi^{(j\ell)}][B_j][[T^{(\ell)}]^{-1}]^* \tag{18}$$

in which

$$[\overset{*}{B}_j] = [B_j]_{,x}\overset{*}{x}(x_j, y_j) + [B_j]_{,y}\overset{*}{y}(x_j, y_j) \tag{19}$$

$$[[T^{(\ell)}]^{-1}]^* = -[T^{(\ell)}]^{-1}[\overset{*}{T}^{(\ell)}][T^{(\ell)}]^{-1} \tag{20}$$

$$[\overset{*}{T}^{(\ell)}] = [T^{(\ell)}_{gh,n_x}\overset{*}{n}_x + T^{(\ell)}_{gh,n_y}\overset{*}{n}_y + T^{(\ell)}_{gh,x}\overset{*}{x} + T^{(\ell)}_{gh,y}\overset{*}{y}] \tag{21}$$

($T^{(\ell)}_{gh}$ are the components of matrix $[T^{(\ell)}]$, n_x and n_y are the components of the outward normal vector to ∂B), and the components of matrix $\overset{*}{\Phi}^{(j\ell)}$ are given by (let $z = h + 10(k-1)$ where $h = 1, \ldots, 10$)

$$\begin{aligned}
\overset{*}{\phi}^{(j\ell)}_{ki} &= \overset{*}{\phi}_z(\xi_{\ell 2}, \eta_{\ell 2}) - \overset{*}{\phi}_z(\xi_{\ell 1}, \eta_{\ell 1}) \\
&= \frac{\partial \phi_z(\xi_{\ell 2}, \eta_{\ell 2})}{\partial \xi}[\overset{*}{x}(x_{\ell 2}, y_{\ell 2}) - \overset{*}{x}(x_j, y_j)] + \frac{\partial \phi_z(\xi_{\ell 2}, \eta_{\ell 2})}{\partial \eta}[\overset{*}{y}(x_{\ell 2}, y_{\ell 2}) - \overset{*}{y}(x_j, y_j)] \\
&\quad - \frac{\partial \phi_z(\xi_{\ell 1}, \eta_{\ell 1})}{\partial \xi}[\overset{*}{x}(x_{\ell 1}, y_{\ell 1}) - \overset{*}{x}(x_j, y_j)] - \frac{\partial \phi_z(\xi_{\ell 1}, \eta_{\ell 1})}{\partial \eta}[\overset{*}{y}(x_{\ell 1}, y_{\ell 1}) - \overset{*}{y}(x_j, y_j)].
\end{aligned} \tag{22}$$

The potential functions ϕ_z are listed in the Appendix of the paper by Phan *et al.* (1997a) and the determination of their gradients $\partial\phi_z/\partial\xi$ and $\partial\phi_z/\partial\eta$ are also addressed in that paper. It should be noted that $\partial\phi_z/\partial\xi$ and $\partial\phi_z/\partial\eta$ are singular when $Q(x_\ell, y_\ell) \to P(x_j, y_j)$, i.e. when $(\xi, \eta) \to (0, 0)$, but in this case $[\overset{*}{x}(x_\ell, y_\ell) - \overset{*}{x}(x_j, y_j)] = [\overset{*}{y}(x_\ell, y_\ell) - \overset{*}{y}(x_j, y_j)] \sim O(r)$, thus, unlike $[\Phi^{(j\ell)}]$, the matrix $[\overset{*}{\Phi}^{(j\ell)}]$ is completely regular.

The advantage of the equality $[\overset{*}{\Psi}^{(j\ell)}] = [\overset{*}{\Phi}^{(j\ell)}]$ lies in the fact that the evaluation of $[\overset{*}{\Phi}^{(j\ell)}]$ is more convenient than that of $[\overset{*}{\Psi}^{(j\ell)}]$ and the expression (22) can be reused in the computation of DSCs in the domain B^*, as discussed later in this paper.

Displacement continuity across elements is now applied to system (15) which results in the new system of equations

$$[\overset{*}{M}^{(j)}]\{p\} + [M^{(j)}]\{\overset{*}{p}\} = \{0\} \tag{23}$$

where $\{p\}$ and $\{\overset{*}{p}\}$ are the degrees-of-freedom (DOF) and their sensitivities, respectively, on the whole boundary ∂B.

With $2n$ source points corresponding to $2n$ displacement nodes on the boundary ∂B in the numerical implementation using quadratic boundary elements, one gets $2n$ relations of the form (23) which are now combined into the following linear system

$$[\overset{*}{M}]\{p\}+[M]\{\overset{*}{p}\}=\{0\}. \tag{24}$$

System (24) needs to be split in accordance with the boundary conditions to yield

$$[\overset{*}{A}]\{X\}+[\overset{*}{B}]\{Y\}+[A]\{\overset{*}{X}\}+[B]\{\overset{*}{Y}\}=\{0\} \tag{25}$$

where $\{X\}$ and $\{Y\}$ contain, respectively, the unknown and known (from boundary conditions) physical quantities. It is noted that, at this stage, $\{X\}$ is known from the solution of the BCM system $[A]\{X\}=\{Z\}$, where $\{Z\}=[B]\{Y\}$. Furthermore, it is assumed that the boundary conditions are kept fixed during the change of the design variables, so that $\{\overset{*}{Y}\}=\{0\}$. By shifting the known terms to the right-hand side, eqn (25) becomes

$$[A]\{\overset{*}{X}\}=-[\overset{*}{B}]\{Y\}-[\overset{*}{A}]\{X\} \tag{26}$$

or

$$[A]\{\overset{*}{X}\}=\{W\}. \tag{27}$$

This final linear system is very similar to the BCM system $[A]\{X\}=\{Z\}$. The matrix $[A]$ is identical in both equations. Also, it is generally overdetermined, but always consistent and, therefore, the rectangular system solving algorithm used to solve the usual BCM equations, can be reused here.

3.3. *Displacement sensitivities in the domain* B*

The displacement in the domain B^* is evaluated from eqn (3) which can now be written as [see Phan *et al.* (1997a)]

$$\gamma\{u_k(\mathbf{b},P)\}=\left\{\sum_{\ell=1}^{n}[\Phi_k^{(\ell)}(E_{\ell 2})-\Phi_k^{(\ell)}(E_{\ell 1})]\right\}=\sum_{\ell=1}^{n}[\Phi^{(P\ell)}][B_P]\{\beta^{(\ell)}\} \tag{28}$$

where $\gamma=0.5$ if the source point P (where displacements are to be computed) is on the boundary ∂B^* and $\gamma=1$ if P is inside the body B.

Thus, displacement sensitivities in the domain B^* can be found by differentiating eqn (28) with respect to a design variable b. That means

$$\gamma\{u_k(\mathbf{b},P)\}^*=\sum_{\ell=1}^{n}\{[\overset{*}{\Phi}^{(P\ell)}][B_P]\{\beta^{(\ell)}\}+[\Phi^{(P\ell)}][\overset{*}{B}_P]\{\beta^{(\ell)}\}+[\Phi^{(P\ell)}][B_P]\{\overset{*}{\beta}^{(\ell)}\}\} \tag{29}$$

in which $[\overset{*}{B}_P]$ and $[\overset{*}{\Phi}^{(P\ell)}]$ are computed by using eqns (19) and (22), respectively, and since $\{\beta^{(\ell)}\}=[T^{(\ell)}]^{-1}\{p^{(\ell)}\}$ [see (10)], one gets

$$\{\overset{*}{\beta}^{(\ell)}\}=[[T^{(\ell)}]^{-1}]^*\{p^{(\ell)}\}+[T^{(\ell)}]^{-1}\{\overset{*}{p}^{(\ell)}\} \tag{30}$$

where $[[T^{(\ell)}]^{-1}]^*$ is determined by eqn (20) and $\{\overset{*}{p}^{(\ell)}\}$ is known at this stage after the solution of (27) because $\{\overset{*}{p}^{(\ell)}\}$ is derived from $\{\overset{*}{p}\}$ which is formed from $\{\overset{*}{X}\}$ with $\{\overset{*}{Y}\}=\{0\}$.

3.4. *Stress sensitivity recovery at boundary traction and endpoint nodes*

Stresses can be calculated using Hooke's law

$$\sigma_{ij}=\lambda\delta_{ij}u_{k,k}+\mu(u_{i,j}+u_{j,i}) \tag{31}$$

where λ and μ are Lamé constants of the material, δ_{ij} is the Kronecker delta ($\equiv 1$ for $i=j$ and $\equiv 0$ for $i\neq j$).

The stress sensitivities are determined by taking the total derivative of eqn (31) with respect to a design variable b to yield

$$\overset{*}{\sigma}_{ij} = \lambda\delta_{ij}(u_{k,k})^* + \mu[(u_{i,j})^* + (u_{j,i})^*]. \tag{32}$$

In order to evaluate (recover) the stress sensitivities at traction nodes where the traction sensitivities are available after the solution of eqn (27), their displacement gradient tensor used in (31) needs to be computed first. It starts from the displacement shape functions (9) whose displacement gradient tensor is given by

$$\{u^{(\ell)}\}_{,m} = [T_u^{(\ell)}(x, y)]_{,m}\{\beta^{(\ell)}\} \tag{33}$$

where m is a field point index for the coordinate system (x, y), i.e. $_{,1} \equiv \partial/\partial x$ and $_{,2} \equiv \partial/\partial y$.

Finally, the sensitivity of the displacement gradient tensor required by eqn (32) is derived from eqn (33)

$$\{\{u^{(\ell)}\}_{,m}\}^* = [[T_u^{(\ell)}(x, y)]_{,m}]^*\{\beta^{(\ell)}\} + [T_u^{(\ell)}(x, y)]_{,m}\{\overset{*}{\beta}{}^{(\ell)}\} \tag{34}$$

in which $\{\overset{*}{\beta}{}^{(\ell)}\}$ is evaluated using eqn (30).

The above approach is equivalent to the stress recovery procedure in the usual BEM [see, for example, Kane and Saigal (1988)], but more straightforward, since the global displacement shape functions (9) are employed in the BCM. For computing stress sensitivities at endpoint nodes, the problem is much easier if the starting point is the displacement expression (11). In this case, the displacement gradients at an endpoint node are, simply:

$$\langle u_{1,1}^{(\ell)}\ u_{1,2}^{(\ell)}\ u_{2,1}^{(\ell)}\ u_{2,2}^{(\ell)}\rangle^{\mathrm{T}} = \langle \hat{\beta}_2^{(\ell)}\ \hat{\beta}_3^{(\ell)}\ \hat{\beta}_5^{(\ell)}\ \hat{\beta}_6^{(\ell)}\rangle^{\mathrm{T}} \tag{35}$$

where (ℓ) is the element containing this endpoint node so that its coordinates are $(\xi, \eta) = (0, 0)$. Therefore, the sensitivity of the displacement gradients required by eqn (32) is

$$\langle (u_{1,1}^{(\ell)})^*\ (u_{1,2}^{(\ell)})^*\ (u_{2,1}^{(\ell)})^*\ (u_{2,2}^{(\ell)})^*\rangle^{\mathrm{T}} = \langle \overset{*}{\hat{\beta}}{}_2^{(\ell)}\ \overset{*}{\hat{\beta}}{}_3^{(\ell)}\ \overset{*}{\hat{\beta}}{}_5^{(\ell)}\ \overset{*}{\hat{\beta}}{}_6^{(\ell)}\rangle^{\mathrm{T}} \tag{36}$$

in which the components on the right-hand side of eqn (36) are derived from the sensitivity of eqn (12), i.e from

$$\{\overset{*}{\hat{\beta}}{}^{(\ell)}\} = [\overset{*}{B}_j]\{\beta^{(\ell)}\} + [B_j]\{\overset{*}{\beta}{}^{(\ell)}\}. \tag{37}$$

The above procedure from eqn (32) to eqn (34) is simple and it can be used to compute the stress sensitivities on the whole boundary ∂B. Stress sensitivities in the domain B^* can be computed by using the direct formulation addressed in the following section.

3.5. *Stress sensitivities in the domain* B*

This kind of sensitivity is also computed using eqn (32). To this end, the first step is to determine the displacement gradient tensor $u_{i,j}$ on the body B^* by taking the partial derivative of eqn (28) with respect to a source point P [see Phan *et al.* (1997a)] to yield

$$\gamma\{u_{k,M}(\mathbf{b}, P)\} = \sum_{\ell=1}^{n} ([\Phi^{(P\ell)}][B_P]_{,M} - [\Phi^{(P\ell)}]_{,\mu}[B_P])\{\beta^{(\ell)}\} \tag{38}$$

where M is a source point index for the coordinate system (x, y), i.e. $_{,1} \equiv \partial/\partial x(P)$ and

$_{,2} \equiv \partial/\partial y(P)$, and μ is a field point index for the coordinate system (ξ, η), i.e. in this case $_{,1} \equiv \partial/\partial\xi$ and $_{,2} \equiv \partial/\partial\eta$.

Then, the sensitivity of the displacement gradient tensor is derived from (38) to give

$$\gamma\{u_{k,M}(\mathbf{b}, P)\}^* = \sum_{\ell=1}^{n} ([\overset{*}{\Phi}{}^{(P\ell)}][B_P]_{,M} + [\Phi^{(P\ell)}][[B_P]_{,M}]^* - [[\Phi^{(P\ell)}]_{,\mu}]^*[B_P]$$

$$- [\Phi^{(P\ell)}]_{,\mu}[\overset{*}{B}_P])\{\beta^{(\ell)}\} + \sum_{\ell=1}^{n} ([\Phi^{(P\ell)}][B_P]_{,M} - [\Phi^{(P\ell)}]_{,\mu}[B_P])\{\overset{*}{\beta}{}^{(\ell)}\}. \quad (39)$$

In eqn (39)

$$[[B_P]_{,M}]^* = \begin{cases} \dfrac{\partial^2[B_P]}{\partial x^2}\overset{*}{x}(x_P, y_P) + \dfrac{\partial^2[B_P]}{\partial x\,\partial y}\overset{*}{y}(x_P, y_P) & \text{if } M = 1 \\ \dfrac{\partial^2[B_P]}{\partial x\,\partial y}\overset{*}{x}(x_P, y_P) + \dfrac{\partial^2[B_P]}{\partial y^2}\overset{*}{y}(x_P, y_P) & \text{if } M = 2 \end{cases} \quad (40)$$

and the components of matrix $[[\Phi^{(P\ell)}]_{,\mu}]^*$ are given by

$$(\phi_{ki,\mu})^* = (\phi_{z,\mu}(\xi_{\ell 2}, \eta_{\ell 2}))^* - (\phi_{z,\mu}(\xi_{\ell 1}, \eta_{\ell 1}))^* \quad (41)$$

in which

$$(\phi_{z,\mu}(\xi_\ell, \eta_\ell))^* = \begin{cases} \dfrac{\partial^2\phi_z(\xi_\ell, \eta_\ell)}{\partial\xi^2}[\overset{*}{x}(x_\ell, y_\ell) - \overset{*}{x}(x_P, y_P)] \\ + \dfrac{\partial^2\phi_z(\xi_\ell, \eta_\ell)}{\partial\xi\,\partial\eta}[\overset{*}{y}(x_\ell, y_\ell) - \overset{*}{y}(x_P, y_P)] & \text{if } M = 1 \\ \dfrac{\partial^2\phi_z(\xi_\ell, \eta_\ell)}{\partial\xi\,\partial\eta}[\overset{*}{x}(x_\ell, y_\ell) - \overset{*}{x}(x_P, y_P)] \\ + \dfrac{\partial^2\phi_z(\xi_\ell, \eta_\ell)}{\partial\eta^2}[\overset{*}{y}(x_\ell, y_\ell) - \overset{*}{y}(x_P, y_P)] & \text{if } M = 2. \end{cases} \quad (42)$$

It can be seen from eqn (41) that in order to calculate $[[\Phi^{(P\ell)}]_{,\mu}]^*$, one needs to evaluate the second-order gradient of the potential functions ϕ_z, i.e. $\partial^2\phi_z/\partial\xi^2$, $\partial^2\phi_z/\partial\eta^2$ and $\partial^2\phi_z/\partial\xi\,\partial\eta$. Three points need to be mentioned with regard to the evaluation of displacement and stress sensitivities on the boundary ∂B^*.

- As demonstrated in the work by Phan *et al.* (1997a), unlike the conventional BEM, eqns (28) and (38) are completely regular when they are used to calculate displacements and stresses on the boundary ∂B^*. This advantage allows one to derive formulae for the corresponding DSCs directly, as presented above. In the usual BEM, a similar procedure for computing the stress sensitivities on the boundary was presented by Barone and Yang (1988), but the formula involves strongly singular integrals. An approximate formula was introduced in the above work in order to overcome the difficulty.
- When the source point P lies on the boundary ∂B^*, the evaluation of matrix $[\Phi^{(P\ell)}]$ has to be carried out carefully by using the approach addressed in the earlier work by Phan *et al.* (1997a).
- The matrix $[\Phi^{(P\ell)}]$ is singular when the source point P (where the DSCs are to be computed) approaches an endpoint node. Thus, eqns (29) and (39) are only used for calculating DSCs in the domain B^* where endpoint nodes are excluded. However,

the displacement and stress sensitivities at endpoint nodes can be obtained from the equations in Sections 3.2 and 3.4, respectively.

4. NUMERICAL EXAMPLES

Three examples are illustrated in this section. The same material data for all these examples are as follows: Young's modulus $E = 2.5$ (in consistent units) and Poisson's ratio $v = 0.3$.

4.1. *Lamé's problem*

Consider a thick cylinder subjected to uniform pressure p_i on the inner surface. Let a and b be the inner and outer radii of the cylinder where a is chosen as the design variable.

The analytical expressions in polar coordinates (r, θ), for the displacement and stress fields of Lamé's problem, are available from Timoshenko and Goodier (1970). In the case of a plane stress state

$$u_r = \frac{a^2 p_i}{E(b^2 - a^2)}\left[(1-v)r + (1+v)\frac{b^2}{r}\right]$$

$$\sigma_{r/\theta} = \frac{a^2 p_i}{b^2 - a^2}\left(1 \mp \frac{b^2}{r^2}\right) \tag{43}$$

in which, the expressions for σ_r and σ_θ correspond to the upper and lower signs respectively.

By assuming that the geometry changes linearly with the changes of the design variable a, one gets $\overset{*}{r} = (b-r)/(b-a)$ (Chandra and Mukherjee, 1997). So, the analytical sensitivity fields are found by taking the total derivative of eqn (43) with respect to the design variable a (using eqn (16) written in polar coordinates) to give

$$\overset{*}{u}_r = \frac{a^2 p_i}{E(b^2 - a^2)}\left[\frac{2b^2}{b^2 - a^2}\left\{(1-v)r + (1+v)\frac{b^2}{r}\right\} + \frac{a(b-r)}{b-a}\left\{1 - v - (1+v)\frac{b^2}{r^2}\right\}\right]$$

$$\overset{*}{\sigma}_{r/\theta} = \frac{2ab^2 p_i}{r^2(b^2 - a^2)}\left[\frac{r^2 \mp b^2}{b^2 - a^2} \pm \frac{a(b-r)}{r(b-a)}\right]. \tag{44}$$

Because of the symmetry of the problem, only a quarter of the structure needs to be modeled as shown in Fig. 2. The mesh consists of equal numbers of quadratic boundary elements on each segment of the boundary. Also, all the elements on a given segment are of equal length. In general, a finer mesh ensures better convergence of numerical results, and especially, in the calculation of displacement sensitivities. Figures 3–6 display numerical results obtained by using a total of 60 quadratic elements. Excellent agreement with the analytical solutions is seen. Figures 3 and 4 show numerical results for the DSCs on the boundary AB (see Fig. 2), in which, the approach presented in Section 3.4 is employed to recover the stress sensitivities in Fig. 4. Finally, the formulas in Section 3.3 and 3.5 are used to compute the displacement sensitivities (Fig. 5) and the stress sensitivities (Fig. 6) on the line segment IJ (see Fig. 2) (domain B^*), respectively.

4.2. *Kirsch's problem*

The second example deals with Kirsch's problem. Figure 7 shows a quarter symmetry model of a square plate with a central circular hole of radius a subjected to a unit uniaxial tensile load S. The stress components in polar coordinates (r, θ) are given by Timoshenko and Goodier (1970) as

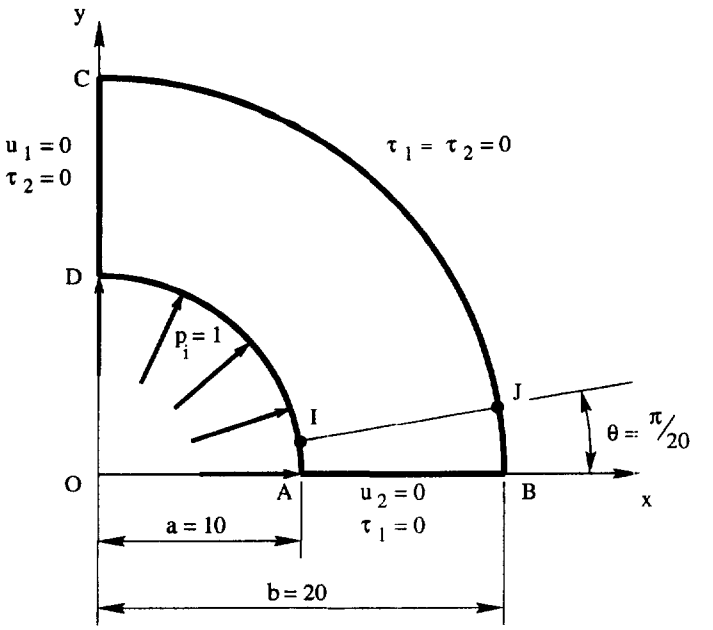

Fig. 2. Modeling of Lamé's problem.

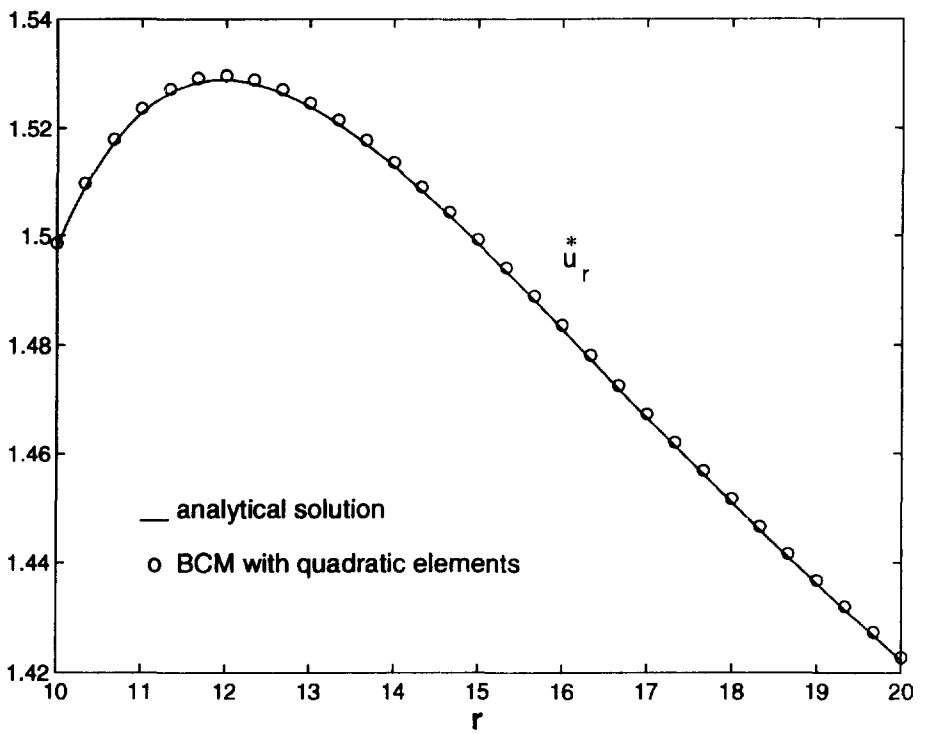

Fig. 3. Displacement sensitivity on the edge AB (see Fig. 2).

$$\sigma_r = \frac{S}{2}\left(1-\frac{a^2}{r^2}\right)+\frac{S}{2}\left(1+\frac{3a^4}{r^4}-\frac{4a^2}{r^2}\right)\cos 2\theta$$

$$\sigma_\theta = \frac{S}{2}\left(1+\frac{a^2}{r^2}\right)-\frac{S}{2}\left(1+\frac{3a^4}{r^4}\right)\cos 2\theta$$

$$\tau_{r\theta} = -\frac{S}{2}\left(1-\frac{3a^4}{r^4}+\frac{2a^2}{r^2}\right)\sin 2\theta. \tag{45}$$

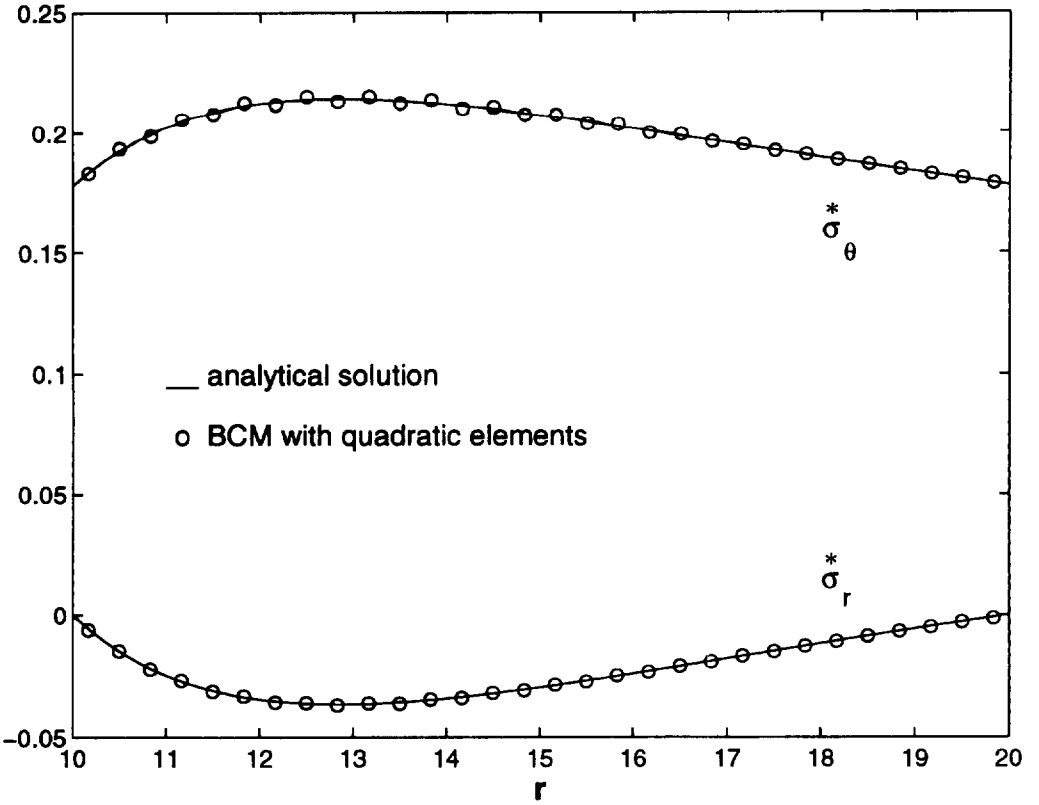

Fig. 4. Stress sensitivities on the edge AB (see Fig. 2).

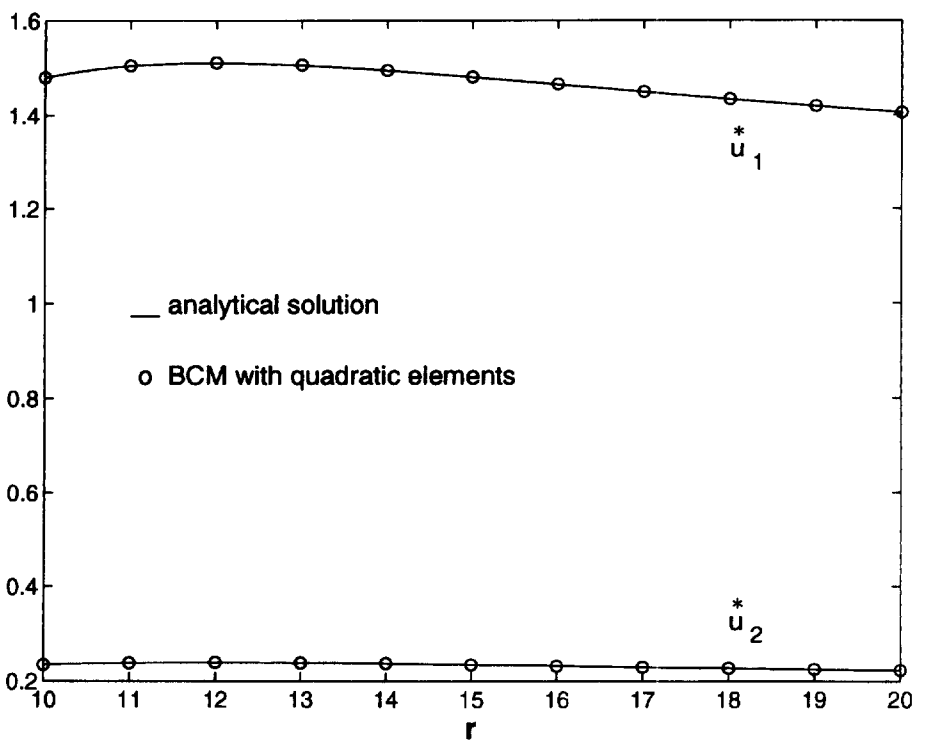

Fig. 5. Displacement sensitivities along the line IJ (see Fig. 2).

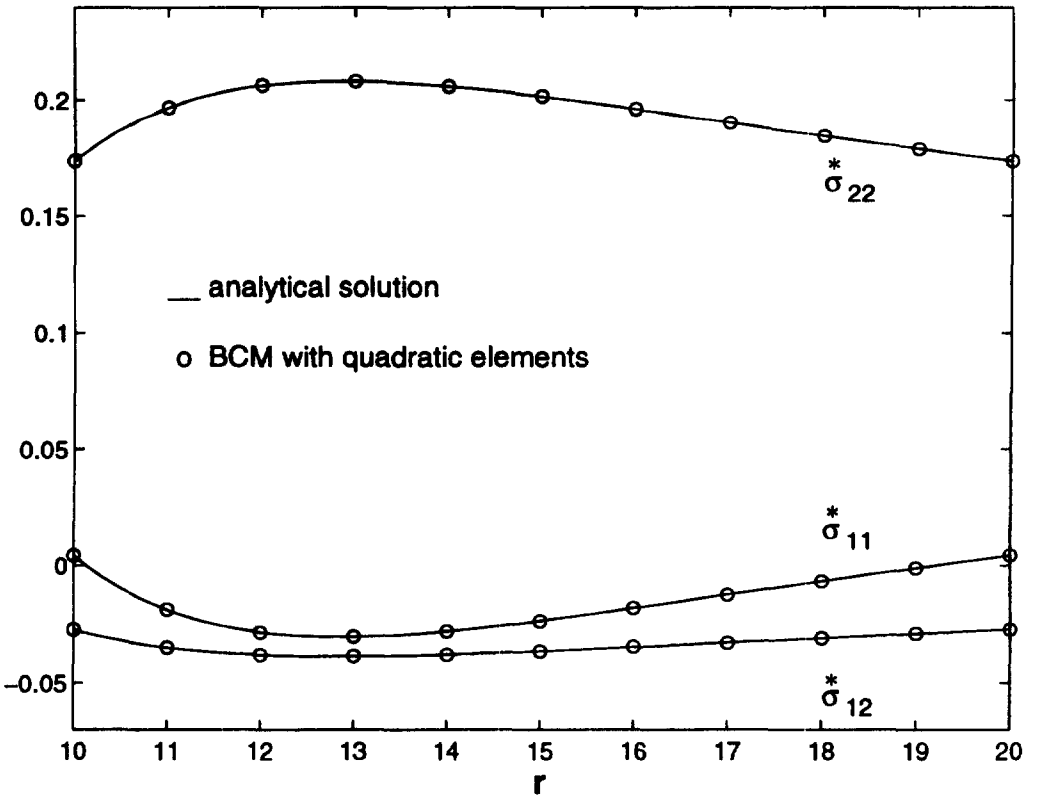

Fig. 6. Stress sensitivities along the line *IJ* (see Fig. 2).

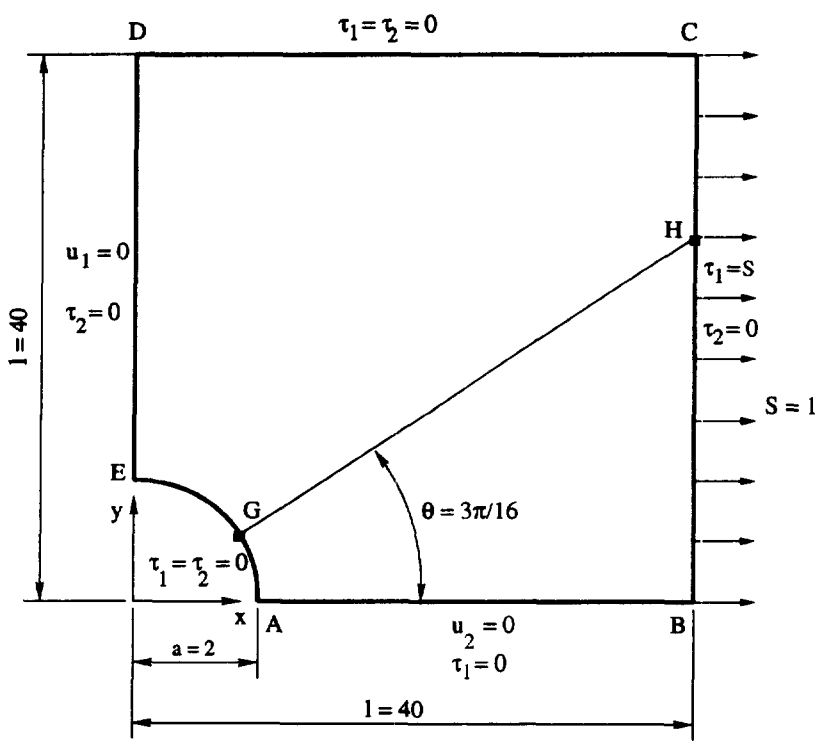

Fig. 7. Modeling of Kirsch's problem.

Here, a is chosen as the design variable. The total derivative of eqn (45) is obtained using the same approach as in the previous example to yield the stress sensitivity fields where, with the same linear assumption as in Lamé's problem, the geometric sensitivities are given by

$$\left.\begin{aligned} \overset{*}{r} &= \frac{l-r}{l-a} \quad \text{if } r \leqslant l \\ \overset{*}{r} &= 0 \qquad \text{if } r > l \end{aligned}\right\}. \tag{46}$$

The boundary contour analysis model is made up of 34 quadratic elements: 10 elements on the edges AB and DE, four elements on the edges BC and CD, and six elements on the arc EA (see Fig. 7). Due to stress concentrations at the corners A and E, the mesh in this zone needs to be refined: the density of elements on AB and DE is nonuniform, with short elements being placed near the points A and E.

The numerical results for the stress sensitivities on the boundary DE, computed from the approach presented in Section 3.4, are shown in Figs 8 and 9. For the stress sensitivities in the domain B^* (along the line segment GH, see Fig. 7), a state of plane stress is employed to analytically compute the sensitivity of the von Mises stress. The von Mises stress and its sensitivity are:

$$\begin{aligned} \sigma_{\mathrm{VM}} &= \sqrt{\sigma_{11}^2+\sigma_{22}^2+3\sigma_{12}^2-\sigma_{11}\sigma_{22}} \\ \overset{*}{\sigma}_{\mathrm{VM}} &= \frac{(2\sigma_{11}-\sigma_{22})\overset{*}{\sigma}_{11}+(2\sigma_{22}-\sigma_{11})\overset{*}{\sigma}_{22}+6\sigma_{12}\overset{*}{\sigma}_{12}}{2\sigma_{\mathrm{VM}}}. \end{aligned} \tag{47}$$

Analytical and numerical results for this quantity are presented in Fig. 10. This time, the formulas in Sections 3.3 and 3.5 are used. Reasonably good agreements with the analytical solutions are observed, even though the analytical solutions exhibit some rapid changes along the lines DE and GH in Fig. 7.

4.3. *Infinite plate with an elliptical hole*

Infinite plates with elliptical holes, subjected to uniform biaxial tensions S_1 and S_2, are studied in this example. Because of symmetry, only a quarter of a plate needs to be modeled

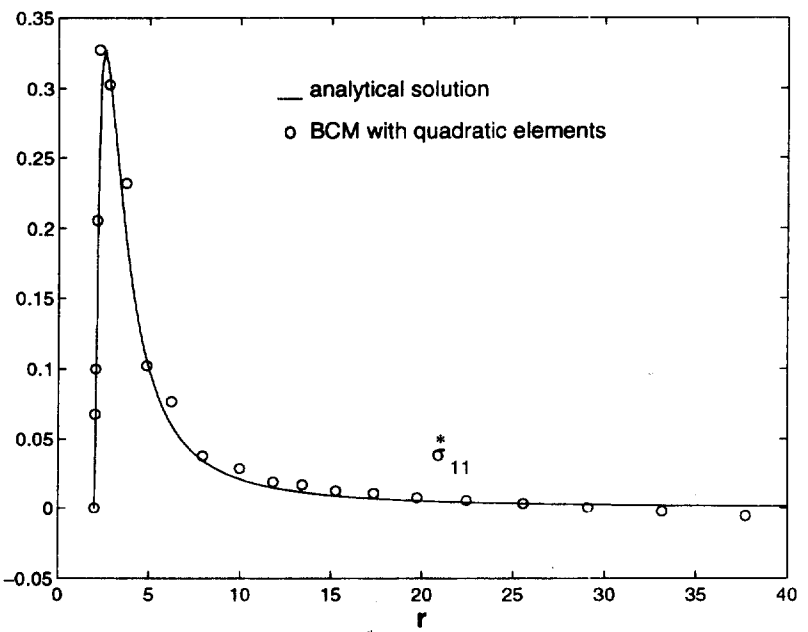

Fig. 8. Stress sensitivity $\overset{*}{\sigma}_{11}$ on the edge DE (see Fig. 7).

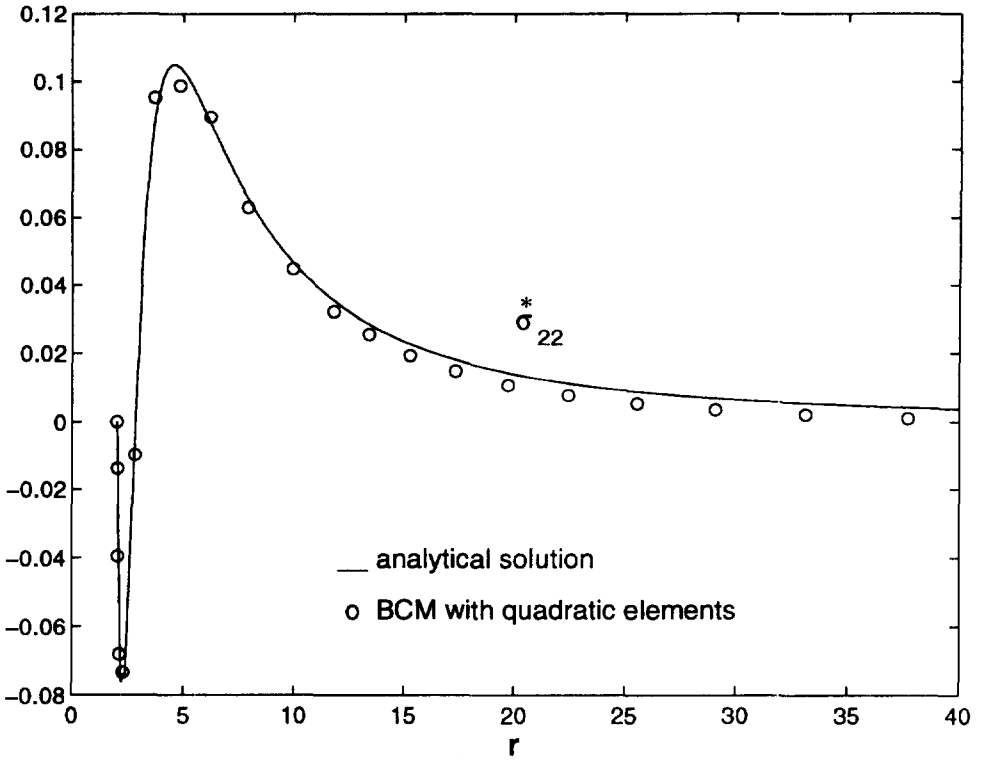

Fig. 9. Stress sensitivity $\overset{*}{\sigma}_{22}$ on the edge DE (see Fig. 7).

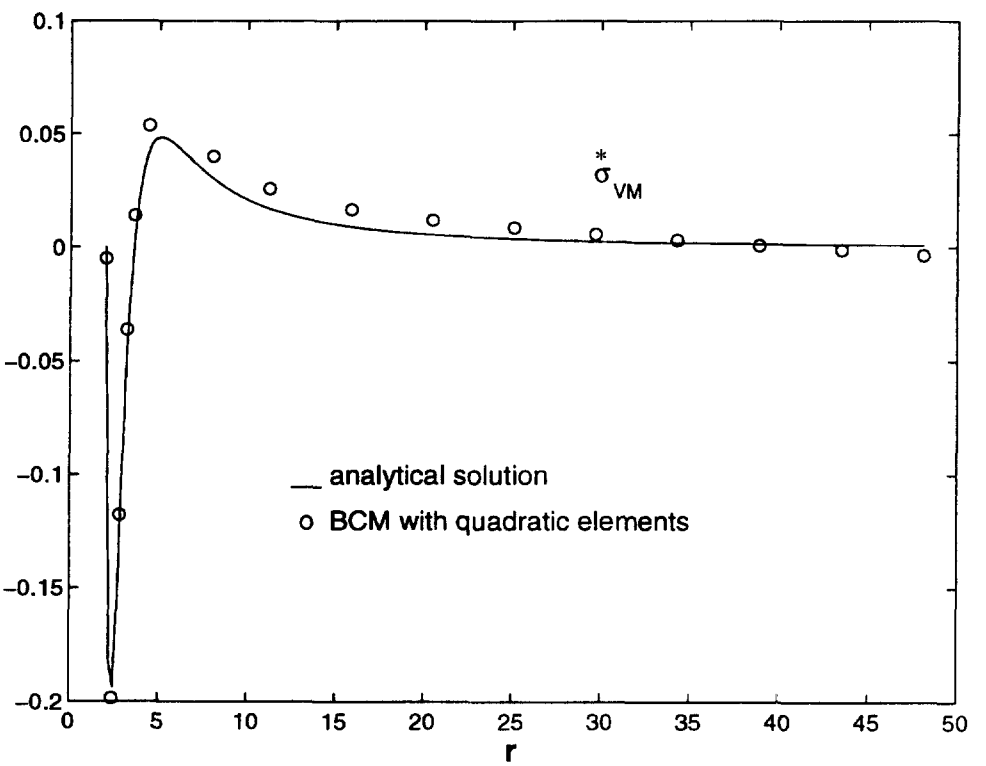

Fig. 10. Sensitivity of the von Mises stress along the line GH (see Fig. 7).

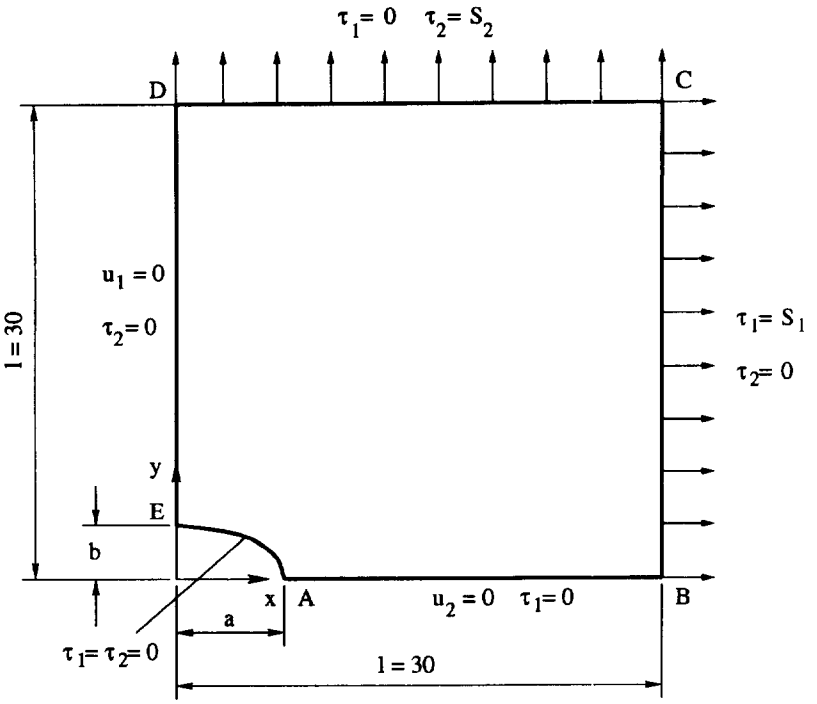

Fig. 11. Modeling of a plate with an elliptical hole.

as shown in Fig. 11. Let a and b be, respectively, the semi-major and semi-minor axes of the hole. Two cases are considered here:

(a) $S_1 = 0$, $S_2 = 1$, $a = 2$ and $b = 1$ in which a is chosen as the design variable. The same data as in the work of Zhang and Mukherjee (1991) (where the derivative BEM was employed) are used here for the purpose of comparison. Graded meshes with 11 elements each are used on each of the sides AB and DE (due to the stress concentration at A), uniform discretizations (with four elements each) are used on each of the sides BC and CD, and 10 elements are placed at equal increments of the eccentric angle ϕ on the elliptical arc EA.

The focus here is on the tangential ("skin") stress σ_s on the hole boundary since it is often used as a control parameter in shape design. The analytical solution for σ_s, and its sensitivity for this case, are presented by Barone and Yang (1988).

Numerical and analytical solutions are compared in Figs 12 and 13. It is quite remarkable that the results given from the BCM are seen to have excellent agreement with the exact solution on the entire elliptical hole boundary. Furthermore, Fig. 13 also shows that the present formulation yields better results than those obtained from the BEM by Zhang and Mukherjee (1991). Only very slight numerical oscillations are seen in this figure even though fewer quadratic elements (especially only a half of elements on the elliptical boundary) are employed in this BCM study, as opposed to the previous BEM research. In this work there are 11 elements on each of the segments AB and DE and 10 on EA, compared to 12, 14 and 20, respectively, in the BEM work of Zhang and Mukherjee (1991).

(b) $S_1 = 1$, $S_2 = 0.75$ for $\beta = b/a = 0.5$, 0.75 and 1, respectively. The mesh is the same as in the previous case, except that 12 elements each are used on each of the sides AB and DE, and 20 elements are spaced around the arc EA.

The analytical solutions for the stress sensitivities at the points A and E are given by Barone and Yang (1988)

$$a\overset{*}{\sigma}_{22}(A) = -\frac{1.5}{\beta^2}$$

$$a\overset{*}{\sigma}_{11}(E) = 2. \tag{48}$$

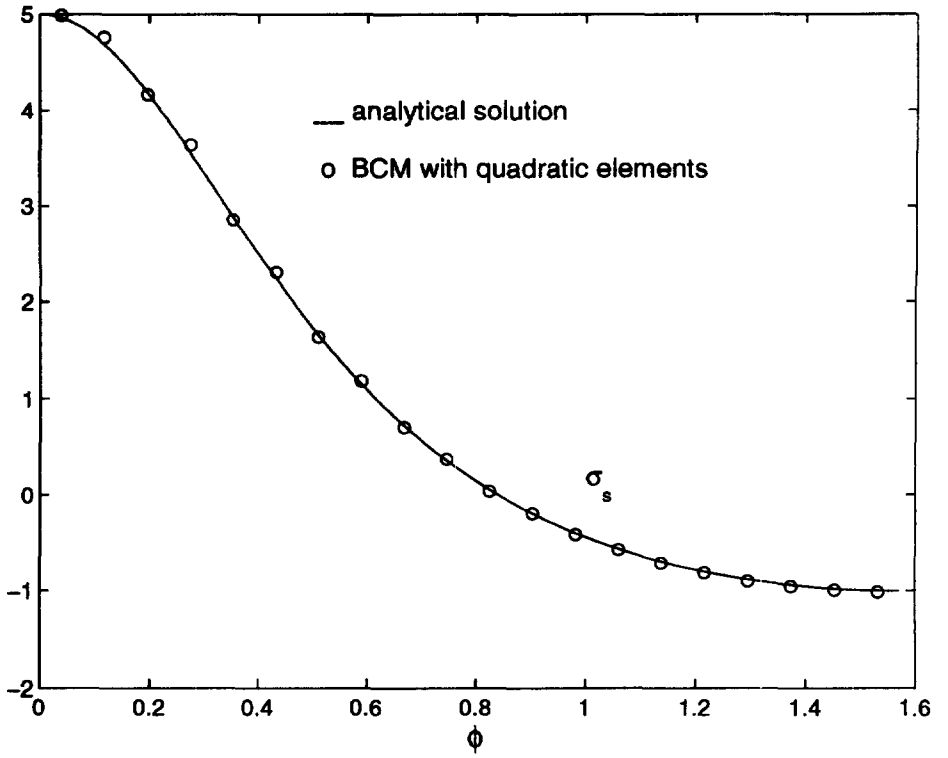

Fig. 12. "Skin" stress σ_s on the arc EA (see Fig. 11).

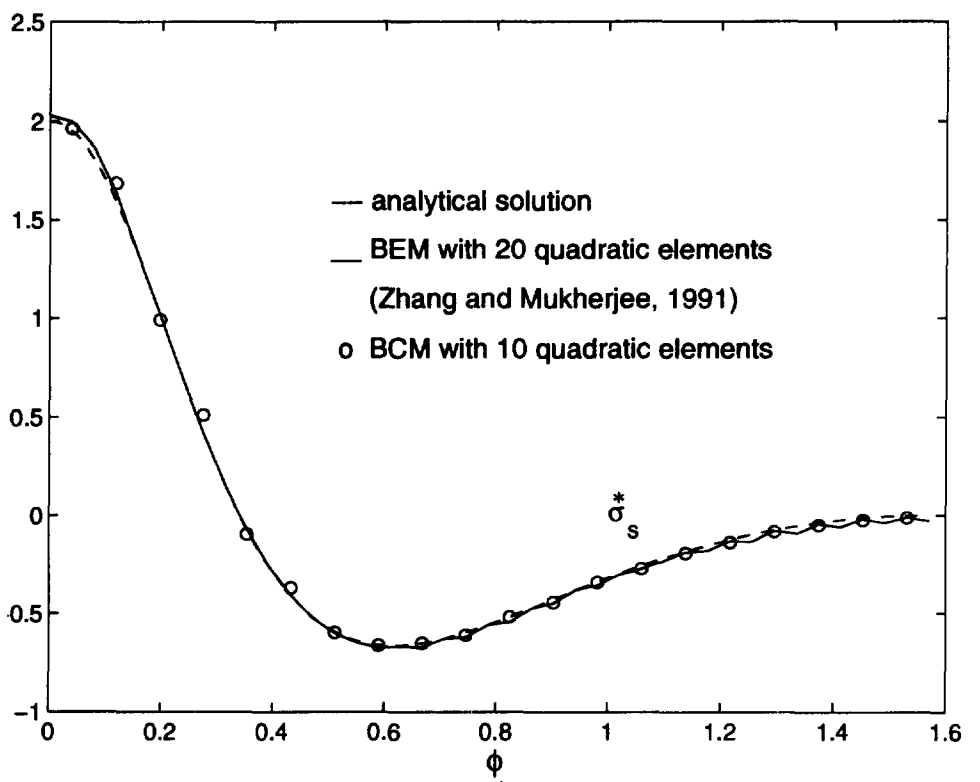

Fig. 13. "Skin" stress sensitivity $\overset{*}{\sigma}_s$ on the arc EA (see Fig. 11).

Table 1. Stress sensitivities at A and E (Fig. 11) for different values of β

	$a\overset{*}{\sigma}_{22}(A)$			$a\overset{*}{\sigma}_{11}(E)$		
β	Analytical	BCM	BEM	Analytical	BCM	BEM
0.5	−6	−5.996	−6.158	2	1.992	2.247
0.75	−2.667	−2.662	−2.983	2	1.992	2.339
1	−1.5	−1.506	−1.828	2	1.994	2.540

Table 1 shows the analytical values of these quantities together with the numerical results obtained by this work (BCM) as well as by the BEM (Chandra and Mukherjee, 1997). It should be noted that in the BCM, numerical results for stresses (and thus, stress sensitivities) are discontinuous at endpoint nodes. Although this is a minor drawback, it makes the modeling of corners trivial. At endpoint nodes on which the stresses from the analytical solution are continuous, the discontinuity magnitudes produced by the BCM are minor. Hence, it is reasonable to use the average values as final outputs. This kind of output is shown in the Table 1 as the numerical results from the BCM. Again, these results are in excellent agreement with the analytical ones, and the performance of the BCM in design sensitivity analysis appears to be much superior to the BEM in this example.

5. CONCLUSIONS

A formulation for design sensitivity analysis by the BCM for 2-D linear elasticity is presented in this paper. An implementation is carried out with quadratic boundary elements.

The present formulation deals with the calculation of DSCs throughout the domain of interest, i.e. on the boundary ∂B as well as inside the body B. Since global displacement and stress shape functions are used in the BCM, the nodal stress sensitivities can be recovered in a straightforward manner from these functions and from the results obtained after solving the system (27). For evaluating displacement and stress sensitivities in the domain B^*, direct formulas are developed from the corresponding nonsingular expressions for displacements and stresses in the domain given in Phan *et al.* (1997a).

It is quite remarkable that the accuracy of numerical results for illustrative problems is seen to be very high. It is felt that the primary reason for this is the complete absence of numerical integration in the BCM for 2-D problems. Another possible reason is that the global displacement shape functions satisfy, *a priori*, the Navier–Cauchy equilibrium equations (Phan *et al.*, 1997a). Accuracy and efficiency in design sensitivity analyses are crucial since they lead to faster convergence of iterative procedures in shape optimization.

The DDA developed in this work is advantageous for optimal shape design problems with few design variables and a large number of constraints. For problems involving many design variables and fewer constraints, the ASA is more suitable. The ASA, based on the BCM, is an important subject for future research.

Acknowledgements—Anh-Vũ Phan acknowledges the financial support from the Quebec Ministry of Education through the "Programme québécois de bourses d'excellence".

REFERENCES

Aithal, R., Saigal, S. and Mukherjee, S. (1991) Three dimensional boundary element implicit differentiation formulation for design sensitivity analysis. *Mathematics and Computational Modelling* **15,** 1.

Banerjee, P. K. (1994) *The Boundary Element Methods in Engineering*. McGraw-Hill, Maidenhead, Berkshire, U.K.

Barone, M. R. and Yang, R. J. (1988) Boundary integral equations for recovery of design sensitivities in shape optimization. *AIAA Journal* **26,** 589.

Bonnet, M. (1995) Regularized BIE formulations for first- and second-order shape sensitivity of elastic fields. *Computers and Structures* **56,** 799.

Bui, H. D. and Bonnet, M. (1995) Unknown or variable domains, inverse problems. *Engineering Analysis with Boundary Elements* **15** (special issue).

Chandra, A. and Mukherjee, S. (1997) *Boundary Element Methods in Manufacturing*. Oxford University Press, Oxford.

Haug, E. J., Choi, K. K. and Komkov, V. (1986) *Design Sensitivity Analysis of Structural Systems*. Academic Press, New York.

Kane, J. H. and Saigal, S. (1988) Design sensitivity analysis of solids using BEM. *ASCE Journal of Engineering Mechanics* **114,** 1703.

Kane, J. H., Zhao, G., Wang, H. and Guru Prasad, K. (1992) Boundary formulations for three-dimensional continuum structural shape sensitivity analysis. *ASME Journal of Applied Mechanics* **59,** 827.

Mellings, S. C. and Aliabadi, M. H. (1995) Flaw identification using the boundary element method. *International Journal for Numerical Methods in Engineering* **38,** 399.

Mukherjee, S. (1982) *Boundary Element Methods in Creep and Fracture*. Elsevier Applied Science, London.

Mukherjee, S. and Chandra, A. (1991) A boundary element formulation for design sensitivities in problems involving both geometric and material nonlinearities. *Mathematical Computational Modelling* **15,** 245.

Mukherjee, S. and Mukherjee, Y. X. (1977) The hypersingular boundary contour method for three-dimensional linear elasticity (submitted).

Nagarajan, A., Lutz, E. D. and Mukherjee, S. (1994) A novel boundary element method for linear elasticity with no numerical integration for two-dimensional and line integrals for three-dimensional problems. *ASME Journal of Applied Mechanics* **61,** 264.

Nagarajan, A., Lutz, E. D. and Mukherjee, S. (1996) The boundary contour method for three-dimensional linear elasticity. *ASME Journal of Applied Mechanics* **63,** 278.

Phan, A. V., Mukherjee, S. and Mayer, J. R. R. (1997a) The boundary contour method for two-dimensional linear elasticity with quadratic boundary elements. *Computational Mechanics* (in press).

Phan, A. V., Mukherjee, S. and Mayer, J. R. R. (1997b). The hypersingular boundary contour method for two-dimensional linear elasticity. Submitted to *Acta Mechanica*.

Rice, J. R. and Mukherjee, S. (1990) Design sensitivity coefficients for axisymmetric elasticity problems by boundary element methods. *Engineering Analysis with Boundary Elements* **7,** 13.

Rizzo, F. J. (1967) An integral equation approach to boundary value problems of classical elastostatics. *Quarterly of Applied Mathematics* **25,** 83.

Saigal, S., Borggaard, J. T. and Kane, J. H. (1989) Boundary element implicit differentiation equations for design sensitivities of axisymmetric structures. *International Journal of Solids and Structures* **25,** 527.

Sokolowski, J., Zolesio, J. P. (1992) *Introduction to shape optimization. Shape sensitivity analysis*. Springer series in Computational Mathematics, Vol. 16, Springer-Verlag, Berlin.

Timoshenko, S. P. and Goodier, J. N. (1970) *Theory of Elasticity*. McGraw-Hill, New York.

Zhang, Q. and Mukherjee, S. (1991) Design sensitivity coefficients for linear elastic bodies with zones and corners by the derivative boundary element method. *International Journal of Solids and Structures* **27,** 983.